

## Formation of single-domain anatase $\text{TiO}_2(001)-(1 \times 4)$ islands on $\text{SrTiO}_3(001)$ after thermal annealing

Fabien Silly<sup>a)</sup> and Martin R. Castell<sup>b)</sup>

Department of Materials, University of Oxford, Parks Road, Oxford OX1 3PH, United Kingdom

(Received 7 May 2004; accepted 12 August 2004)

Scanning tunneling microscopy is used to investigate the appearance of nanoscale islands on the  $\text{SrTiO}_3(001)$  surface following cycles of repetitive annealing. Atomic-resolution images reveal that the surface of the islands is covered by features typical of the anatase  $\text{TiO}_2(001)$  surface reconstruction. Small islands display a mixed  $(1 \times 4)$  and  $(1 \times 5)$  reconstruction, whereas only the single-domain  $(1 \times 4)$  reconstruction is observed on large islands. These results reveal a simple process for the creation of single-domain anatase nanoislands. © 2004 American Institute of Physics. [DOI: 10.1063/1.1805177]

Nanostructured  $\text{TiO}_2$  has been extensively studied as a promising material for applications in sensors, photocatalysis, solar energy conversion, and optical coatings. The properties of titania are determined by the crystallographic phase of its polytypes: anatase (tetragonal), brookite (orthorhombic), and rutile (tetragonal). Several techniques are currently used for the production of nanostructured  $\text{TiO}_2$ : sol-gel processing,<sup>1</sup> physical and chemical vapor deposition,<sup>2,3</sup> hydrolysis,<sup>4</sup> and colloidal chemistry methods.<sup>5</sup> The performance of devices made from these materials are strongly dependent on the nature of the  $\text{TiO}_2$  surfaces and its nanostructures. The realization of a substrate covered with  $\text{TiO}_2$  nanodots with a defined shape and single  $\text{TiO}_2$  phase remains an exciting challenge.<sup>6</sup>

In this letter, we show the development of a method for the creation of  $\text{TiO}_2$  surface nanostructures. This is achieved by changing the near-surface stoichiometry of  $\text{SrTiO}_3$  crystals through sputtering and annealing in UHV, which results in the epitaxial growth of nanoscale single-domain reconstruction anatase islands.

Of the perovskite compounds,  $\text{SrTiO}_3$  has been one of the most widely studied due to its technological applications in functional electroceramic devices and as a substrate for the growth of high  $T_c$  cuprate superconductors and metal or semiconductor thin films. The  $\text{SrTiO}_3(001)$  surface presents a multitude of different reconstructions depending on sample preparation.<sup>7–11</sup> Of particular relevance to the present study is the nanostructured  $\text{SrTiO}_3(001)-(6 \times 2)$  surface, which appears to be the necessary precursor structure to the formation of anatase nanoislands. Nb-doped  $\text{SrTiO}_3$  single crystals with epipolished (001) surfaces were supplied by PI-KEM, Surrey, UK. The 0.5% molar Nb content is necessary to allow sufficient electrical conductivity for scanning tunneling microscopy (STM) experiments on a material that has a 3.2 eV bandgap and is hence a good insulator in its pure state. Samples were introduced into the UHV chamber of an STM (JEOL JSTM4500S) operating at a pressure of  $10^{-8}$  Pa. Etched tungsten tips were used to obtain constant current images at room temperature with a bias voltage applied to the sample. The  $\text{SrTiO}_3$  samples were sputtered with 3-keV

argon ions and subsequently annealed in UHV in cycles at 875 °C. The total anneal period was 20 h.

Figure 1 shows the morphology of the  $\text{SrTiO}_3(001)$  surface following sputtering after several annealing cycles at a temperature of 875 °C. The surface is covered by nanostructures which we have described previously and give rise to a  $(6 \times 2)$  reconstruction.<sup>11</sup> In addition, Fig. 1 shows a type of nanoline that causes local  $(9 \times 2)$  ordering, and which we will report on separately.<sup>12</sup> Of interest for this letter is the circled nanoisland, which is different in structure from the surrounding material. Parallel rows are visible on the top of the island that are oriented along one of the  $\langle 100 \rangle$  directions of the  $\text{SrTiO}_3(001)$  surface.

An atomically resolved STM image of a nanoisland similar to that shown in Fig. 1 is presented in Fig. 2(a). The height of the island is 8 Å with respect to the  $\text{SrTiO}_3$  surface. Line scans from Fig. 2(a) are taken along a line perpendicular to the bright rows (A), parallel to the bright rows (C), and between the rows (B). The rows on the cluster surface are separated by 15.2 or 19.5 Å and their height is about 1.7 Å [Fig. 2(b)]. From line scans (B) and (C) [Fig. 2(c)], we find the same periodicity of 3.8 Å along the bright rows (C) and between the rows (B).

The sample was then annealed at 1200 °C for 1 h. The STM images of the surface show that the nanostructures covering the surface disappeared as previously reported in Ref.

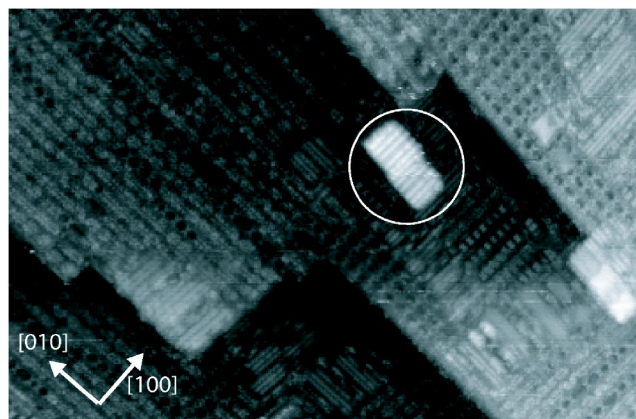


FIG. 1. STM image of an anatase  $\text{TiO}_2$  island on the nanostructured  $\text{SrTiO}_3$  surface ( $100 \times 65 \text{ nm}^2$  image size;  $U_s = +0.8 \text{ V}$ ,  $I_s = 0.3 \text{ nA}$ ).

<sup>a)</sup>Electronic mail: fabien.silly@materials.oxford.ac.uk

<sup>b)</sup>Electronic mail: martin.castell@materials.oxford.ac.uk

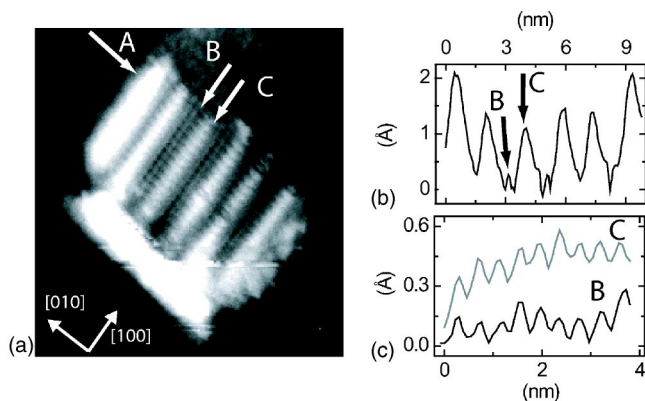


FIG. 2. (a) STM image of an anatase  $\text{TiO}_2$  island ( $14 \times 15 \text{ nm}^2$  image size;  $U_s = +0.8 \text{ V}$ ,  $I_s = 0.3 \text{ nA}$ ). (b) A line trace perpendicular to the rows shows a spacing of 15.2 and 19.5 Å. (c) Line traces parallel to the rows show corrugation periods of 3.8 Å measured on the row (gray) and between the rows (black).

11, but we also found large rectangular islands with parallel rows, as shown in Fig. 3. The island sizes are  $110 \times 95 \text{ nm}^2$  [Fig. 3(a)] and  $110 \times 70 \text{ nm}^2$  [Fig. 3(b)]. A screw dislocation was visible on the top surface of each island observed, as illustrated by Figs. 3(a)–3(c). Only one reconstructed domain per island is observed along one of the  $\langle 100 \rangle$  directions of the  $\text{SrTiO}_3(001)$  surface. Parallel rows covering the surface are separated by 15.2 Å and the corrugation height of the rows is about 2 Å. We never obtained atomically resolved STM images of the surfaces of these large islands. However, STM images show defects along the rows, as shown in Figs. 3(c) and 3(e). The majority of defects are resolved as a dip of 0.6 Å along the row, but some of them were measured at 1.2 Å. The line scan perpendicular to the emerging step at the cluster surface due to a screw dislocation reveals a step height of  $\sim 4.7 \text{ Å}$  [Figs. 3(c) and 3(d)].

Previous experiments have shown that after  $\text{Ar}^+$  ion sputtering and annealing at 875 °C, nanolines and nanodot arrays almost entirely cover the  $\text{SrTiO}_3(001)$  surface. Nanolines appear as double rows<sup>11</sup> or triple rows<sup>12</sup> oriented in the  $\langle 100 \rangle$  directions. The nanolines can adopt a close packing arrangement in which the minimum periodicity is approximately 24 Å (double row) and 36 Å (triple row), which is equivalent to a separation of six and nine unit cells, respectively. The cubic unit cell parameter for  $\text{SrTiO}_3$  is 3.905 Å. The nanolines themselves have a periodicity of 8 Å along their length equivalent to two bulk unit cells, and a surface coverage of a mixed  $(6 \times 2)$  and  $(9 \times 2)$  reconstruction is formed. The close packing of nanolines is a distinctly different structure from the reconstruction formed on the top of the nanoislands discussed here, which can be assigned as a  $(1 \times 4)$  reconstruction (Fig. 3) or local  $(1 \times 5)$  reconstruction (Fig. 2). As this structure was not observed on the  $\text{SrTiO}_3(001)$  surface, but only on the top of islands, we can conclude that the islands have a different chemical composition or crystal structure from the substrate.

Epitaxial, stoichiometric anatase  $\text{TiO}_2$  thin films of high crystalline quality can be grown on  $\text{SrTiO}_3(001)$  through chemical vapor deposition (CVD) and molecular-beam epitaxy (MBE).<sup>2,3</sup> The  $\text{SrTiO}_3(001)$  surface shows a poor lattice match with the rutile phase, but an excellent match with the anatase (001) surface. Anatase  $\text{TiO}_2$  has a tetragonal unit cell within which each Ti atom is coordinated to six oxygen at-

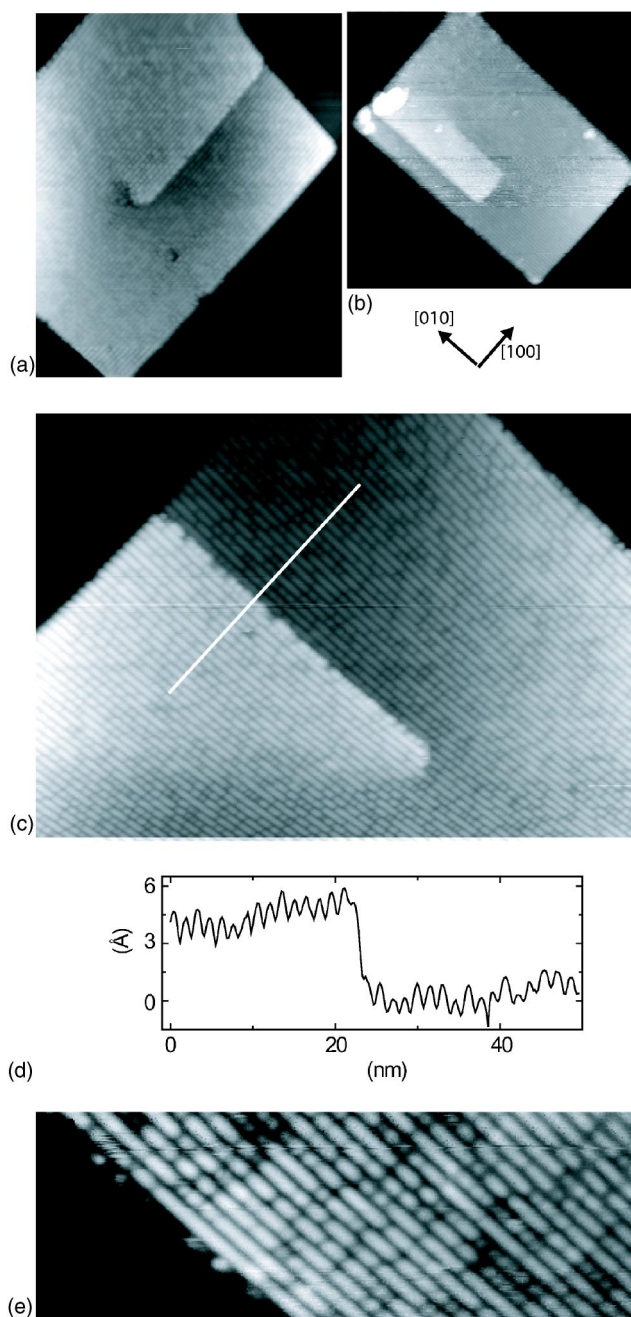


FIG. 3. STM images of large anatase  $\text{TiO}_2$  islands. Image dimensions in (a) are  $100 \times 120 \text{ nm}^2$ , and in (b) are  $130 \times 120 \text{ nm}^2$ . In (c) the  $(1 \times 4)$  reconstruction on the  $\text{TiO}_2$  island can be seen (image size  $100 \times 70 \text{ nm}^2$ ). (d) Line profile perpendicular to the step edge caused by the screw dislocation in (c). (e) High-resolution image of the  $(1 \times 4)$  surface showing a variety of defects ( $50 \times 20 \text{ nm}^2$ ;  $U_s = +4 \text{ V}$ ,  $I_s = 0.3 \text{ nA}$ ).

oms. The anatase unit cell contains 12 atoms and has a volume of  $3.78 \times 3.78 \times 9.51 \text{ Å}^3$ . The nonpolar and autocompensated (001) surface of an anatase film can present a  $(1 \times 4)$  reconstruction as displayed by STM and atomic force microscopy imaging.<sup>13,14</sup> The surface consists of atomic rows separated by  $\sim 16 \text{ Å}$ , corresponding to a  $(1 \times 4)$  reconstruction. Local  $(1 \times 5)$  reconstructions were also sometimes observed as well as atomic corrugations along the rows with a periodicity of  $\sim 4 \text{ Å}$ . Additional faint rows were observed (between bright rows), whose periodicity was  $\sim 4 \text{ Å}$ . It was shown that in a multidomain structure the "lower" terrace can be reproduced from an "upper" terrace by a single-height vertical translation (2.4 Å), accompanied by a 90° rotation



along the [001] axis. The corrugation of the brighter atomic rows along the [100] direction was typically about 1.5 Å measured by STM. The similarity between these observations and the properties of the nanoislands reported here is evident. We find the same atomic periodicity of 4 Å along the bright row and faint row, and the same bright row separation ( $1 \times 4$ ) and ( $1 \times 5$ ), (Fig. 2). The step height observed in Figs. 3(c) and 3(d) is consistent with a double/single-height translation ( $\sim 4.7$  Å). The anatase  $\text{TiO}_2(001)$ -( $1 \times 4$ ) reconstruction has been interpreted using first-principles density functional calculations.<sup>15</sup> The resulting "added molecule" (ADM) model was obtained by periodically adding rows of  $\text{TiO}_2$  molecules to the flat unreconstructed surface. The structure was optimized and the surface energy of various ADM-( $1 \times n$ ) reconstructions ( $n=3-6$ ) was determined. It appears that the ( $1 \times 4$ ) periodicity is indeed the most favorable. The second lowest energy structure has the ( $1 \times 5$ ) periodicity, but the predicted surface energy differences are very small, consistent with the experimental observation by STM of small regions with different periodicities, as we observed in Fig. 2(a). Density of states modeling shows that the bright and faint rows in an STM image correspond to Ti(4) fourfold and Ti(5) fivefold coordinated surface atoms, respectively.

The anionic sublattices of  $\text{SrTiO}_3(001)$  and an anatase  $\text{TiO}_2(001)$  film bear substantial resemblance despite their overall crystallographic dissimilarities. Heteroepitaxial growth of anatase  $\text{TiO}_2$  can be regarded as a continuous formation and extension of the oxygen atom network from the  $\text{SrTiO}_3$  substrate into the anatase island. The oxygen sublattice in anatase is bcc, while in  $\text{SrTiO}_3$  it is also bcc but with a superstructure of oxygen vacancies. Within this oxygen sublattice the (relatively small) Ti cations arrange themselves in their appropriate sites. Formation of interfaces where the oxygen sublattice continues and the metal cation sublattice changes abruptly is often exploited for thin-film heteroepitaxy of metal oxides.<sup>16</sup>

In the observations reported here we show that the repeated annealing at 875 °C of the nanostructured  $\text{SrTiO}_3(001)$  surface induces a degeneration of the nanolines covering the surface, which is correlated with the appearance of anatase  $\text{TiO}_2$  islands.  $\text{TiO}_x$  enrichment of the surface region that gives rise to the nanolines is caused by  $\text{Ar}^+$  ion sputtering, which could either cause nonstoichiometry directly by removing more Sr than Ti ions, or alternatively, the disruption that is caused by the sputtering process allows Ti to preferentially segregate to the surface. The process of island formation is most likely due to the generation of excess Ti and O ions from disintegrating nanolines. These Ti and O ions may diffuse on the surface and form small epitaxial islands. Higher temperature annealing normally yields a complete regeneration of the surface with the disappearance of the nanolines,<sup>11</sup> but the possible presence of small anatase

$\text{TiO}_2$  islands on the surface will act as a cornerstone for diffusing Ti and O ions and produce an increase in the  $\text{TiO}_2$  island size, as observed in Figs. 3(a) and 3(b). The presence of a screw dislocation in the island indicates a spiral growth mechanism. The irregular electronic features of the island surface [Figs. 3(c)–3(e)] may be caused by surface or sub-surface defects. Despite these defects, the surface of the large clusters presents high ordering. Previously a two-domain ( $1 \times 4$ ) reconstruction of  $\text{TiO}_2(001)$  films was reported<sup>2</sup> and scanning probe imaging revealed mixing of small domains ( $< 2000 \text{ nm}^2$ ) oriented along the principal axes.<sup>13,14</sup> In comparison, the anatase  $\text{TiO}_2(001)$  island growth proposed here permits surfaces to form that present one single ( $1 \times 4$ ) reconstructed domain of areas up to  $10\,000 \text{ nm}^2$ . We suggest the reason for this difference is that in our experiments we have a very low density of nucleation sites compared with CVD and MBE growth. Once an island has nucleated on the  $\text{SrTiO}_3(001)$  surface it can therefore grow unimpeded, with a single-domain surface reconstruction.

In summary, we show that monodomain thin-film islands can form on  $\text{SrTiO}_3(001)$ -( $6 \times 2$ ) surfaces after annealing. STM images show ( $1 \times 4$ ) and ( $1 \times 5$ ) surface reconstructions on small islands, which is typical of anatase  $\text{TiO}_2(001)$ . Further annealing of the surface results in growth of the islands, which then become exclusively covered in a single-domain ( $1 \times 4$ ) reconstruction. This work describes a method for the creation of what we believe to be anatase thin-film nanoislands and shows how single-domain anatase structures can be created. The results also provide some interesting insights into metal oxide heteroepitaxy.

The authors would like to thank the Royal Society and DSTL for funding and Chris Spencer, JEOL UK, for precious technical support.

<sup>1</sup>P. Lottici, D. Bersani, M. Braghini, and A. Montenero, *J. Mater. Sci.* **28**, 177 (1993).

<sup>2</sup>G. S. Herman and Y. Gao, *Thin Solid Films* **397**, 157 (2001).

<sup>3</sup>S. Chen, M. G. Mason, H. J. Gysling, G. R. Paz-Pajult, T. N. Blanton, K. M. Chen, C. P. Fictorie, W. L. Gladfelter, A. Franciosi, P. I. Cohen, and J. F. Evans, *J. Vac. Sci. Technol. A* **11**, 2419 (1993).

<sup>4</sup>W. F. Zhang, M. S. Zhang, and Z. Yin, *Phys. Status Solidi A* **179**, 319 (2000).

<sup>5</sup>W. Ma, Z. Lu, and M. Zhang, *Appl. Phys. A: Mater. Sci. Process.* **66**, 621 (1998).

<sup>6</sup>P.-L. Chen, C.-T. Kuo, and F.-M. Pan, *Appl. Phys. Lett.* **84**, 3888 (2004).

<sup>7</sup>M. R. Castell, *Surf. Sci.* **505**, 1 (2002).

<sup>8</sup>T. Kubo and H. Nozoye, *Phys. Rev. Lett.* **86**, 1801 (2001).

<sup>9</sup>Q. D. Jiang and J. Zegenhagen, *Surf. Sci.* **425**, 343 (1999).

<sup>10</sup>M. Naito and H. Sato, *Physica C* **229**, 1 (1994).

<sup>11</sup>M. R. Castell, *Surf. Sci.* **516**, 33 (2002).

<sup>12</sup>F. Silly, D. S. Deak, and M. R. Castell (unpublished).

<sup>13</sup>R. E. Tanner, A. Sasahara, Y. Liang, E. I. Altman, and H. Onishi, *J. Phys. Chem. B* **106** 8211 (2002).

<sup>14</sup>Y. Liang and S. A. Chambers, *Phys. Rev. B* **63** 235402 (2001)

<sup>15</sup>M. Lazzeri and A. Selloni, *Phys. Rev. Lett.* **87**, 266105 (2001).

<sup>16</sup>S. A. Chambers, *Surf. Sci. Rep.* **39** 105 (2000).